Native defects and optical properties of Ar ion irradiated ZnO

S. Pal[1], A. Sarkar[2], D. Sanyal[3], T. Rakshit[4], D. Kanjilal[5], P. Kumar[5], S. K. Ray[4], D. Jana[1*]

[1]*Department of Physics, University of Calcutta, 92, Acharya Prafulla Chandra Road, Kolkata 700 009, India*
[2]*Department of Physics, Bangabasi Morning College, 19, R. C. Sarani, Kolkata 700 009, India*
[3]*Variable Energy Cyclotron Centre (VECC), 1/AF, Bidhannagar, Kolkata 700 064, India*
[4]*Department of Physics and Materials Science, Indian Institute of Technology, Kharagpur 721302, India*
[5]*Inter-University Accelerator Centre, P.O. Box 10502, Aruna Asaf Ali Marg, New Delhi 110067, India*

[*]Corresponding author. Tel: (+91) 33 2350 8386; E-mail: djphy@caluniv.ac.in

ABSTRACT

1.2 MeV Argon (Ar) ion irradiation turns white coloured ZnO to yellowish (fluence 1×10^{14} ions/cm^2) and then reddish brown (1×10^{16} ions/cm^2). At the same time the material becomes much more conducting and purely blue luminescent for the highest fluence of irradiation. To get insight on the defects in the irradiated samples Ultraviolet-visible (UV-vis) absorption, Raman, and photoluminescence (PL) spectroscopy and Glancing Angle X-Ray Diffraction (GAXRD) measurements have been carried out. Enhancement of overall disorder in the irradiated samples is reflected from the GAXRD peak broadening. UV-vis absorption spectra of the samples shows new absorption bands due to irradiation. Complete absorption in the blue region of the spectrum and partial absorption in the green and red region changes the sample colour from white to reddish brown. The Raman peak representing wurtzite structure of the ZnO material (~ 437 cm^{-1}) has decreased monotonically with the increase of irradiation fluence. At the same time, evolution of the 575 cm^{-1} Raman mode in the irradiated samples shows the increase of oxygen deficient disorder like zinc interstitials (I_{Zn}) and/or oxygen vacancies (V_O) in ZnO. PL spectrum of the yellow coloured sample shows large reduction of overall luminescence compared to the unirradiated one. Further increase of fluence causes an increase of luminescence in the blue region of the spectrum. The blue-violet emission can be associated with the interstitial Zn (I_{Zn}) related optical transition. The results altogether indicates I_{Zn} type defects in the highest fluence irradiated sample. Large changes in the electrical resistance and luminescent features of ZnO using Ar ion beam provides a purposeful way to tune the optoelectronic properties of ZnO based devices. Copyright © 2015 VBRI press.

Keywords: ZnO; ion beam irradiation; defects; photoluminescence.

S. Pal is a PhD student in the Physics Department, University of Calcutta, Kolkata, India. He is working mainly on defects in ZnO incorporated by ion beam irradiation.

Introduction

Ion irradiation is an efficient tool for controlled modification of material properties [1]. Here, we investigate the effects of 1.2 MeV Ar ion irradiation on polycrystalline Zinc Oxide (ZnO) material. ZnO bears wide direct band gap (~ 3.37 eV at 300 K) and large exciton binding energy (~ 60 meV). Intense photoluminescence (PL) ranging from ultra-violet (UV) to near infrared (NIR)

photon energies is characteristic of ZnO. So ZnO based optoelectronic devices can be operated even beyond room temperature [2]. Furthermore, ZnO is very much radiation hard and subtle effects of ion irradiation can be observed. Altogether, ZnO is an interesting material both from theoretical and technological purposes [3, 4].

It is well known that during the passage of energetic ions inside a solid all possible vacancies and interstitials are produced. Within few ps a fraction of such vacancy-interstitial pairs recombine. This recombination process depends primarily on two factors. First one is the qualitative and quantitative features of generated defects. The second factor is the nature of target material itself. Particularly in ZnO, the defect recovery rate is very high [5]. After the recombination is over, residual defect species either remain isolated or form complexes depending on the local free energy minimization requirements. Thus, several interesting combinations of defects after ion irradiation can occur, particularly in compound semiconductors. Earlier we

have observed several orders of magnitude decrease of ZnO resistance due to Ar ion irradiation [6]. On the contrary, both increase (for low fluence ~ 10^{14} ions/cm^2) and decrease (high fluence ~ 10^{16} ions/cm^2) of resistance has been found due to oxygen ion irradiation [7]. It can be understood that stable defect centers after Ar and O ion irradiation in ZnO are different in nature. Even the stabilized defects are different in 10^{14} and 10^{16} ions/cm^2 fluence regimes for the same ion beam.

In the present work, we have started Ar ion fluence from 10^{14} ions/cm^2 to detect increase of ZnO resistance, if any. Our study presented here along with the earlier findings [6, 7] point out an important way to generate different types of defect centers in ZnO material. Understanding on the nature and role of such defects in ZnO will be helpful for purposeful tailoring of its optical and electronic properties. To note, some recent advances have been achieved in controlling optical and electrical properties of ZnO based devices using energetic ion beams [8, 9].

Experimental

Materials

ZnO powder (99.99%, Sigma-Aldrich, Germany) has been pelletized and then annealed at 500 °C in air for four hours and cooled slowly (60 °C/hr).

Method

Annealed samples have been irradiated with 1.2 MeV Argon ion beam with fluence 1×10^{14} ions/cm^2 and 1×10^{16} ions/cm^2 using Low Energy Ion Beam Facility [10] (LEIBF) at IUAC, New Delhi, India. The absorption spectra of the ZnO samples have been recorded on Perkin–Elmer Lambda 1050 spectroscope in the UV-Visible range. X-ray diffraction pattern have been taken in a Bruker D8 advance diffractometer with Cu K$_\alpha$ lines (1.54 Å). Sheet resistance has been measured by two contacts from the sample surface, made by gold deposition, using Keithley K2000 multimeter and K2400 current source. Photoluminescence (PL) spectra have been taken using JY-Horiba FluoroLog FL3-11 spectrofluorometer. A 450 W xenon lamp (325 nm excitation wavelength) was used for excitation. Raman spectra have been obtained using 532 nm excitation sources (solid state laser source).

Results and discussion

The maximum penetration depth of 1.2 MeV Ar ions in ZnO is ~ 1 μm (found using the Stopping and Range of Ions in Matter (SRIM) code [11]). SRIM analysis also shows that the relative magnitudes of the ion energy deposition in the target (**Fig. 1**). The electronic energy loss (S_e) is more than the nuclear energy loss (S_n) in the first 700 nm of the beam trajectory and in the rest 300 nm path S_n is higher than the S_e (**Fig. 1**). SRIM analysis estimates the number of generated vacancies ~ 2900 vacancies/ion. The result also points out that zinc vacancy (V_{Zn}) formation is more than the oxygen vacancy (V_O) formation inside ZnO due to Ar ion irradiation. However, 99% of produced V_{Zn} s is dynamically recovered whereas V_O s are stable at room temperature [5].
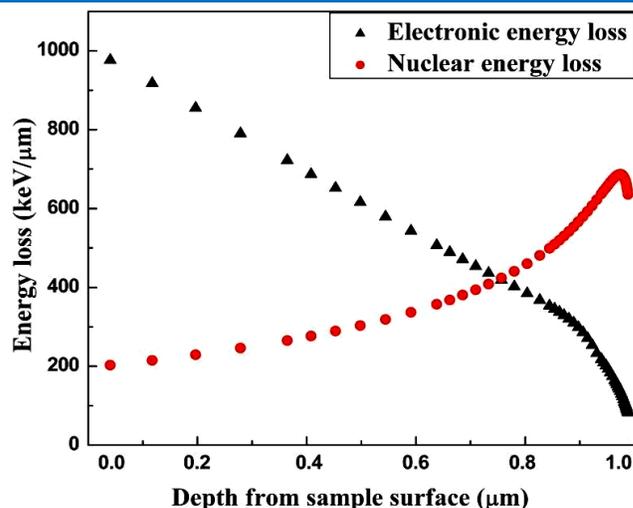
Fig. 1. Energy losses (electronic and nuclear) along with penetration depth (calculated using SRIM code).

After the dynamic recovery of generated defects, residual stable defects play the crucial role in electrical and optical property modification of ZnO. Polycrystalline ZnO pellets generally show very high sheet resistance (~ GΩ/cm^2) which reduces dramatically after high temperature annealing [12]. In the present work, the pristine sample has been pre-annealed at 500 °C and shows sheet resistance ~ 70 MΩ/cm^2. Ar ion irradiation with 1×10^{14} ions/cm^2 fluence increases the sheet resistance by three orders of magnitude. Interestingly, irradiation with 1×10^{16} ions/cm^2 fluence causes a drastic reduction of sheet resistance (in the KΩ/cm^2 range). Such non-monotonic variation of sheet resistance was found by us earlier during oxygen irradiation in ZnO [7] in similar fluence regime. However, reduction of sheet resistance is much more prominent in case of Ar ion beam irradiation. The variation of sheet resistance indicates that the nature of dominant defect types is different in 10^{14} and 10^{16} ions/cm^2 fluence regimes of 1.2 MeV Ar ion irradiated ZnO. To understand this nature of defects, these three samples have been studied from GAXRD, UV-Vis absorption, Raman and PL spectroscopic investigations.
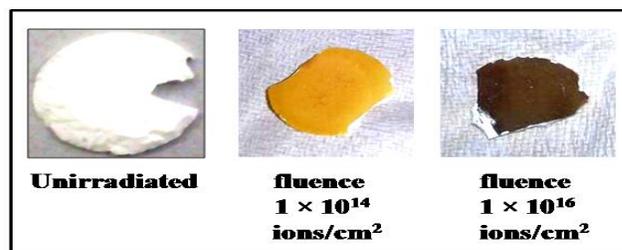
Fig. 2. Colour of the unirradiated and irradiated samples showing the changes in colour due to irradiation.

A significant colour change has been observed in polycrystalline ZnO pellets as an effect of irradiation. White coloured ZnO becomes yellowish after irradiation with low fluence (1×10^{14} ions/cm^2) and it appears as reddish brown in colour with 1×10^{16} ions/cm^2 (**Fig. 2**). This observation is consistent with our UV-Visible absorption spectroscopy results. In **Fig. 3** the absorption

spectra of unirradiated and two irradiated samples are shown (solid line). In the absorption spectra of irradiated samples, a huge tailing in the low energy regime has been observed. To understand this tailing, the difference of the absorption spectra between irradiated and unirradiated samples has been plotted (dashed line) in the same graph.

The difference curve of low fluence absorption spectra clearly shows a broad absorption in blue spectral region with a tailing in green region. This blue absorption can be considered as a single Gaussian peak has peak ~3.05 eV and this absorption is the cause of yellow colouration of low fluence irradiated ZnO. Similar observations have been previously found in electron irradiated [13] and heat-treated ZnO in zinc rich environment [14]. Presence of neutral oxygen vacancies (V_O) can give rise to such an absorption peak in blue region [13, 15]. The absorption extends across blue, green and red spectral region in case of high fluence irradiated spectra and makes the sample reddish brown in colour.
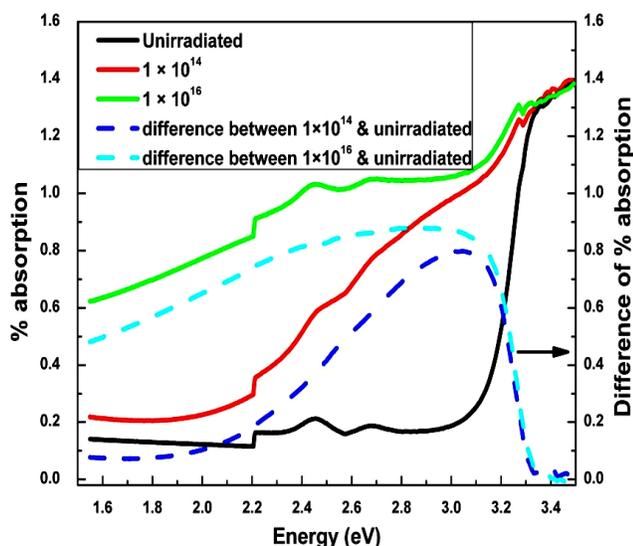
Fig. 3. UV–visible absorption spectra of unirradiated and irradiated ZnO samples.
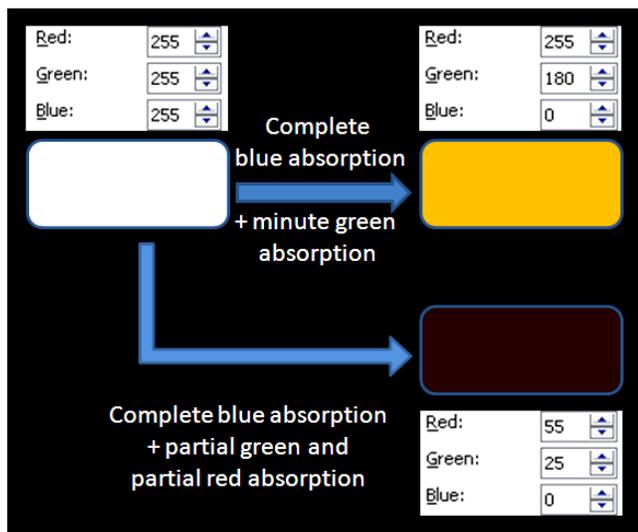
Fig. 4. Schematic representation of different colours of irradiated sample. (colours have been produced using RGB colour model [unit: digital 8 bit per channel]).
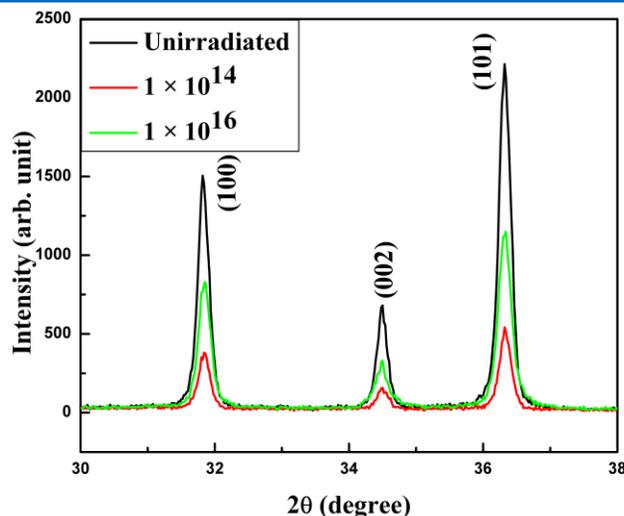
Fig. 5. Glancing angle X-ray diffractogram (GAXRD) of unirradiated and irradiated samples.

Fig. 4 gives a schematic representation by which one can better understand the consistency between UV-Visible absorption spectroscopy result and changes in colour due to irradiation qualitatively. It has been earlier mentioned that 1.2 MeV Ar irradiation causes damage only in sub-surface region (1 μm) in ZnO material. 1.54 Å x-ray probes down to several micrometers [16] of the sample. So, glancing angle XRD (GAXRD) has been used here to probe comparatively larger volume fraction of the irradiated region. In fact, conventional XRD does not detect any change of peak broadening or intensity after irradiation (not shown). **Fig. 5** shows GAXRD of the samples.

Here, decrease of peak intensity after irradiation indicates loss of crystalline nature of the ZnO sample although the decrease is non-monotonic. Such a non monotonic change in peak intensity results from different size of the defect clusters and their spatial separation variation. Similar observation was found in our earlier Ar irradiation work and it has been well discussed in detail [6]. To note, such non-monotonic variation with increasing fluence is also an important key feature of the sheet resistance. The FWHM of the (002) peak has been increased with increasing irradiation fluence. Increase in (002) FWHM indicates that irradiation causes disorder in zinc sublattice [12]. This aspect is important to understand the overall feature of changes in optical and electrical properties of ZnO as we see later on.

Raman spectra of the samples have been shown in **Fig. 6**. The wurtzite structure of ZnO belongs to C_{6V} group. From group theoretical analysis, it was found that the $A_1+E_1+2E_2$ modes are Raman active. Two Raman modes have been observed in unirradiated sample Raman spectra positioned at 100 cm^{-1} [E_2 (low)] and 437 cm^{-1} [E_2 (high)] are characteristic of wurtzite structure. A new broad Raman mode at 575 cm^{-1} [E_1 (LO)] has emerged after irradiation. Besides, the decrease in intensity of E_2 (high) mode has been observed with increasing fluence. The lowering of intensity of E_2 (high) mode can be explained as loss of long range crystalline symmetry which is due to formation of huge lattice defects inside ZnO [asokan + kanjilal]. Evolution of 575 cm^{-1} Raman mode is commonly attributed

as oxygen deficiency i.e. presence of I_{Zn} or V_O or both in ZnO [18].

UV-Visible absorption spectroscopy result and colour change of the sample show that V_O type defect may be present inside sample due to irradiation. **Fig. 7** shows room temperature photoluminescence (PL) spectra of all samples under study. For the unirradiated sample a near band edge (NBE) UV emission (~ 3.27 eV) which is asymmetric in nature and a broad deep level emission (DLE) (~2.13 eV) is observed. After irradiation with 1×10^{14} ions/cm^2 fluence, the overall luminescence (both NBE and DLE) is quenched.
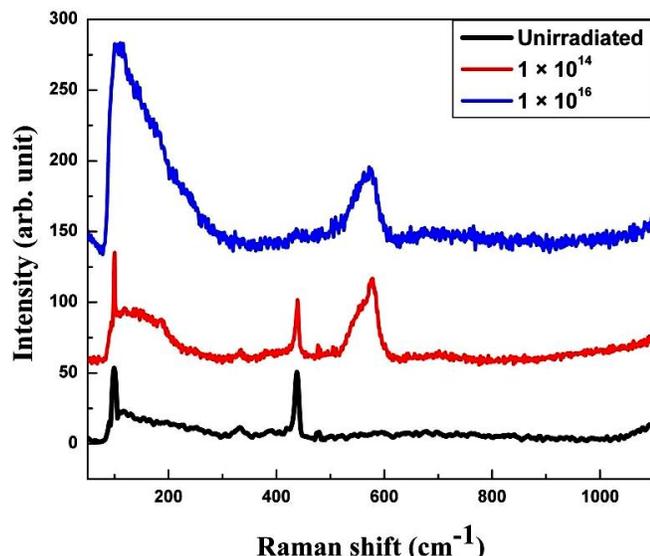
Fig. 6. Raman scattering spectrum of unirradiated and irradiated samples.
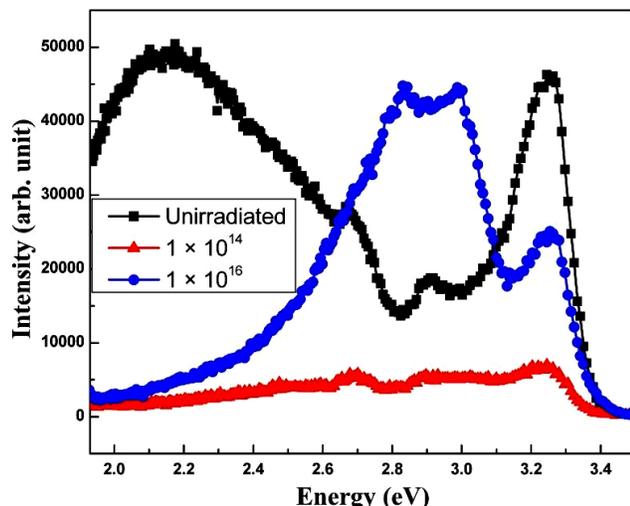
Fig. 7. Photoluminescence spectra of unirradiated and irradiated samples.

Note that, this sample possesses the highest sheet resistance. It may be possible that non-radiative recombination dominates here and isolated V_{Zn} type defects acts as the recombination centre. Appearance of V_{Zn} type defects is also reflected in the GAXRD results. V_{Zn} type defect are compensating acceptors [19] thus 'kill' the donors and make the sample sheet resistance highest. The important fact is that the sample irradiated with 1×10^{16} ions/cm^2 exhibits an intense pure blue-violet emission which is very rare in ZnO. The blue-violet luminescence is pure in the sense that the other luminescence which are

commonly found in ZnO like green luminescence, yellow luminescence are totally suppressed here. This blue-violet luminescence consists of mainly two peaks centered at ~ 2.83 eV (blue emission) and ~ 2.96 eV (violet emission). Based on the previous theoretical calculation and experimental observations, both violet emission (~2.96 eV) and blue emission (~ 2.83 eV) can be related with I_{Zn} type defects [20, 21]. Zeng et al. have shown that the transitions from the I_{Zn} and extended I_{Zn} levels to valence band give violet and blue emission respectively [20]. In general, I_{Zn} is very mobile inside ZnO and so it is really very difficult to stabilize it. However, Kim and Park have shown in their theoretical calculations that when I_{Zn} and V_o are spatially separated below 6 Å helps each other to stabilize [22]. In the light of above theoretical calculations we may assume the strong presence of I_{Zn} - V_o pair in high fluence Ar irradiated ZnO. UV-Visible absorption spectroscopy, colour change of the samples, Raman measurement results are in agreement with the presence of V_o in irradiated ZnO. Kim and Park have also indicated that this I_{Zn}-V_o defect pair is an important source of n-type conductivity in ZnO [22]. Interestingly, sample which exhibits blue – violet emission has the lowest sheet resistance among all the samples. So taking all into account it can be concluded that I_{Zn}-V_o defect pair has been formed in 1×10^{16} ions/cm^2 fluence irradiated sample and played the dominant key role causing low sheet resistance and blue-violet emission. It can also be understood that the sample irradiated at 1×10^{14} ions/cm^2 fluence bear predominantly V_{Zn} type defects. This eventually supports the non-equilibrium origin of these defect centers as claimed by Zeng et al. in laser ablation method [20].

Conclusion

1.2 MeV Ar irradiation on ZnO causes change of colour and huge variation of sheet resistance (both increase and decrease). The colour change in the irradiated samples is related with V_o type defects. The increase in sheet resistance at low fluence regime is due to presence of acceptor like defects (V_{Zn}) which compensates the donors while the formation of I_{Zn}-V_o type defect pair is the cause of decrease in sheet resistance for higher fluence. The highest fluence irradiated sample exhibits blue-violet emission which can be related with I_{Zn} type defects. So it will be interesting to explore such defects responsible for blue-violet emission in ZnO by controlling energy and ion species of irradiation. At the same time Ar beam can be purposefully used to tailor resistance of the ZnO based devices. Further studies are welcome on this regard.

Reference

1. Avasthi, D. K.; Mehta, G. K.; Swift heavy ions for materials engineering and nano-structuring.
   ISBN: 978-94-007-1228-7
2. Margueron, S. and Clarke, D.R.; *J. Appl. Phys.* **2014,** *116*, 193101
   DOI: 10.1063/1.4901833
3. Bang, J.; Kim, Y.S.; Park, C. H.; Gao, F; Zhang, S. B.; *Appl. Phys. Lett.* **2014**, *104*, 252101
   DOI: 10.1063/1.4884653
4. Shukla, S. K.; Vamakshi.; Minakshi.; Bharadavaja, A.; Shekhar, A; Tiwari, A; *Adv. Mat. Lett.* **2012**, *3(5)*, 421
   DOI: 10.5185/amlett.2012.5349
5. Tuomisto, F.; Saarinen, K.; Look, D. C.; Farlow, G. C.; *Phys. Rev. B* **2005**,*72*, 085206
   DOI: 10.1103/PhysRevB.72.085206
6. Chattopadhyay, S.; Dutta, S.; Jana, D.; Chattopadhyay, S. ; Sarkar, A.; *J. Appl. Phys.* **2010,** *107*, 113516
   DOI: 10.1063/1.3429081
7. Pal, S.; Sarkar, A.; Chattopadhyay, S.; Chakrabarti, M.; Sanyal, D.; Kumar, P.; Kanjilal, D.; Rakshit, T.; Ray, S.K.; Jana, D.; *Nucl. Instrum. Meth. B*, **2013**, *311*, 20.
   DOI: 10.1016/j.nimb.2013.06.009
8. Wang, W.; Qi, J.; Qin, Z.; Wang, Q.; Sun, X.; Zhang, Y.; *J. Phys. Chem. C.* **2012,** *116,* 12397
   DOI: 10.1021/jp210934f
9. Ming, X.; Lu, F.; Yin, J.; Chen, M.; Zhang, S.; Liu, X.; Qin, Z.; Ma, Y.; *optics exp.* **2011,** *19(8)*, 7139
   DOI: 10.1364/OE.19.007139
10. Kumar, P.; Rodrigues, G.; Rao, U.K.; Safvan, C.P.; Kanjilal, D.; Roy, A.; *Pramana*, **2002**, *59*, 805
11. Ziegler, J.F.; Biersack, J.P.; Littmark, U.; Stopping Power and Ranges of Ion in Matter, Pergamon, New York, 1985.
12. Dutta,S.; Chattopadhyay,S.; Sarkar, A.; Chakrabarti,M.; Sanyal,D.; Jana, D.; *Prog. Mat. Sci.* **2009,** *54*, 89.
    DOI: 10.1016/j.pmatsci.2008.07.002
13. Kappers, A.; Gilliam, O.R.; Evans, S.M.; Halliburton, L.E.; Giles, N.C.; *Nucl. Instr. Meth. B*, **2008**, *266*, 2953.
    DOI: 10.1016/j.nimb.2008.03.146.
14. Halliburton, L.E.; Giles, N.C.; Garces, N.Y.; Luo, M.; Xu, C.; Bai, L.; Boatner, L.A.; *Appl. Phys. Lett.* **2005**, *87*, 172108
    DOI: 10.1063/1.2117630
15. Anwand, W.; Brauer, G.; Grynszpan, R.I.; Cowan, T.E.; Schulz, D.; Klimm, D.; Cizˇek, J.; Kuriplach, J.; Prochazka, I.; Ling, C.C; Durišic´ , A.B.; Klemm, V.; Schreiber, G.; Rafaja, D.; *J. Appl. Phys.* **2011**, *109*, 063516.
    DOI: 10.1063/1.3559264
16. Sarkar, A.; Chakrabarti,M.;, Bhowmick,D.; Chakrabarti,A.; Ray,S.K.; Rafaja,D.; Sanyal,D.; *J. Phys.: Condens. Matter.* **2013,** *25*, 385501.
    DOI:10.1088/0953-8984/25/38/385501
17. Kumar, S.; Asokan, K.; Singh, R. K.; Chatterjee, S.; Kanjilal, D. Ghosh, A. K.; *RSC Adv.,* **2014**, *4*, 62123
    DOI: 10.1039/C4RA09937K
18. Chen, Z. Q.; Kawasuso, A.; Xu, Y.; Naramoto, H.; Yuan, X. L. ; Sekiguchi, T.; Suzuki, R.; Ohdaira, T.; *J. Appl. Phy.* **2005**, *97,* 013528
    DOI: 10.1063/1.1821636
19. Tuomisto, F.; Ranki, V.; Saarinen, K.; Look, D. C.; *Phys. Rev. Lett.* **2003,** *91*, 205502
    DOI: 10.1103/PhysRevLett.91.205502
20. Zeng, H.; Duan, G.; Li, Y.; Yang, S.; Xu, X.; Cai, W; *Adv. Funct. Mater.* **2010**, *20*, 561
    DOI: 10.1002/adfm.200901884
21. Lin, B.; Fu, Z.; Jia, Y.; *Appl. Phys. Lett.* **2012** *100*, 159902
    DOI: 10.1063/1.1394173
22. Kim, Y.S.; Park, C.H.; *Phys. Rev. Lett.* **2009**, *102*, 086403.
    DOI: 10.1103/PhysRevLett.102.086403